

RESULTS

The median follow-up period was 59.5 months (range, 7.4–122.6 months). The local control rate was 94% (16 of 17 patients) at the last follow-up. The tumor size remained stable in 13 patients and decreased in 3 patients (Fig. 1). No obvious difference was observed between the patients who received radiotherapy after surgery and those initially treated by radiotherapy with respect to both local control and improvement of neurologic symptoms: 85.7% (6 of 7) versus 100% (10 of 10) and 57.1% (4 of 7) versus 50% (5 of 10), respectively. Tumor enlargement with cystic change was seen 12 months after SRT in 1 patient who received 44 Gy in 22 fractions plus 10 Gy in 4 fractions for postoperative recurrence of trigeminal nerve schwannoma. This patient received a salvage operation because the tumor had not decreased in size even at 32 months after SRT. The surgical specimen showed schwannoma cells and cysts with a wall of collagen fiber without evidence of gliosis. There was no relapse after the salvage surgery until she died of gastric carcinoma 92 months after surgery.

Regarding pre-existing neurologic symptoms, 8 of 17 patients (47%) improved and 9 patients remained unchanged. Among the 4 patients with facial nerve schwannomas, none had worsening of their pre-existing neurologic symptoms and 2 patients showed an improvement (Table 1). Temporary nausea, taste change, dizziness, tinnitus, and headache were seen in 5 patient, 3 patients, 2 patients, 1 patient, and 1 patient, respectively. All these patients showed improvement during the follow-up period. No patients had new cranial nerve deficit or other symptomatic adverse effects develop. Intracranial malignant tumor did not develop any patient, suggesting that there was no radiation-induced secondary carcinogenesis during the follow-up period.

DISCUSSION

Stereotactic irradiation by use of precise diagnostic images and accurate fixation has been proven useful to treat intracranial benign tumors. Fractionated radiotherapy is expected to reduce the risk of injury to the surrounding normal structures and to better preserve normal tissue function than single-dose irradiation. It has been reported that SRT is superior to SRS with regard to the preservation of acoustic function (17, 18), and the same may be true for nonacoustic intracranial schwannomas. Fractionated SRT has also been suggested to be more effective for cystic-type schwannomas than SRS (19). In addition, the fractionated radiotherapy does not require an invasive fixation and is more comfortable for the patients than SRS, with the only requirement being that patients are available to visit the clinic frequently.

Zabel *et al.* (20) administered SRT (total dose of 54–57.6 Gy, 5 days per week, with 1.8 Gy per fraction) for 13 nonacoustic intracranial schwannomas (located in the trigeminal nerve in 7 cases, located in the lower cranial nerve origin in 3, and located in the cerebellopontine angle without involvement of the acoustic nerve in 3) from 1996 to 2000. They found that the local control rate was 100% and there was no development of new cranial nerve or brain stem deficits over the median follow-up period of 33 months (range, 13–70 months). Improvement of pre-existing neurologic deficit was seen in 4 patients (31%). The authors concluded that SRT is an effective and well-tolerated noninvasive treatment for nonacoustic intracranial schwannoma, with an excellent tumor control rate.

Our study showed that the local control rate of SRT was 94% (16 of 17 patients) after a median imaging follow-up of 59.5 months. The mean tumor volume was 8.2 mL with a range of 0.3 to 31.3 mL, which is equivalent to the values in the

Table 1. Characteristics of patients with facial nerve schwannoma

Patient no.	Gender	Age (y)	Side	Surgery	Size (mm)	Dose (Gy/fractions/d)	Follow-up (mo)	Tumor size	Symptoms	Adverse effect
6	F	25	Right	None	13 × 13 × 15	50/25/51	61.8	No remarkable change (14 × 13 × 13)	Grade II facial palsy; unchanged after SRT	None
9	F	20	Left	None	9 × 8 × 8	50/25/49	77.7	No remarkable change (11 × 8 × 8)	Grade II facial palsy; subjectively improved after SRT	None
10	F	43	Left	None	5 × 5 × 20	50/25/45	75.7	Decreased (4 × 4 × 10)	Grade II facial palsy; subjectively improved after SRT	None
13	M	26	Right	None	22 × 19 × 20	50/25/45	54.0	Decreased (21 × 15 × 14)	Grade IV facial palsy; unchanged after SRT	Temporal nausea and headache

Abbreviations: F = female; SRT, stereotactic radiotherapy; M = male.

Table 2. Surgical resection, stereotactic radiosurgery, and stereotactic radiotherapy for nonacoustic schwannomas

Series	No. of patients	Tumor size	Follow-up	Local control	Neurologic deficits (patients)	Neurologic improvement (patients)
Surgical resection						
Sanna <i>et al.</i> (7), 2002	46 (V in 26, VII in 7, IX/X/XI in 9, XII in 3, III in 1)	N.R.	Mean, 33.6 mo	100%	New deficits in 11 (24%)	II in 4, III in 5, IV in 2, V in 9, VI in 9, VII in 6, VIII in 6, IX/X/XI in 4
Samii <i>et al.</i> (1, 3), 1995	12 (V)	From 2 × 2 × 3 cm to 4 × 4 × 5 cm	Mean, 25 mo	83%	Temporary paraparesis in 1, temporary facial weakness in 2	N.R.
	16 (IX/X/XI)	From 1 × 1 cm to 6 × 5 cm	Mean, 22 mo	100%	Temporary cranial nerve morbidity in 6 (38%), new deficits in 11 (50%)	N.R.
Sanna <i>et al.</i> (10), 2006	22 (IX/X/XI)	N.R.	Mean, 36.6 mo	100%	Worsened VII in 3, VIII in 2	VII in 1, VIII in 2
Day and Fukushima (21), 1998	38 (V)	N.R.	Mean, 77 mo	97%	New or worsened V in 53%	Diplopia in 4, headache in 5, ataxia in 2
Stereotactic radiosurgery						
Pollock <i>et al.</i> (8), 2002	23 (V in 10, IX/X/XI in 10, XII in 2, IV in 1)	Median prescription isodose volume, 8.9 mL	Median, 43 mo	96%	New or worsened V in 3 (10%)	N.R.
Mabanta <i>et al.</i> (9), 1999	18 (V in 7, VII in 2, IX/X/XI in 9)	Mean volume, 5.5 mL	Mean, 32 mo	100%	Worsening of pre-existing VII palsy in 1 (6%), new onset of hearing loss in 2 (11%)	5 (28%)
Kida <i>et al.</i> (5), 2007	14 (VII)	Mean volume, 5.5 mL	Mean, 31.4 mo	100%	Worsened VII in 1 (7%)	5 (36%)
Litre <i>et al.</i> (11), 2007	11 (VII)	Mean volume, 0.888 mL	Median, 39 mo	91%	Did not worsen in any patient	VII in 3 (27%), balance problems and hearing in 1 (9%)
Huang <i>et al.</i> (12), 1999	16 (V)	Mean volume, 5.3 mL	Mean, 44 mo	100%	Did not observe any new neurologic deficits	5 (31%)
Martin <i>et al.</i> (13), 2007	34 (IX/X/XI)	Median, 4.2 mL	Mean, 83 mo	94%	Worsened in 1 (3%)	20% of affected cranial nerves
Muthukumar <i>et al.</i> (14), 1999	17 (IX/X/XI)	Median tumor diameter, 22.5 mm	Median, 39 mo	94%	Worsened in 1 (8%)	6 (46%)
Stereotactic radiotherapy						
Wallner <i>et al.</i> (22), 1988	18	N.R.	Range, 2–15 y	50%	N.R.	N.R.
Zabel <i>et al.</i> (20), 2001	13 (V in 7, lower cranial nerve in 3, cerebellopontine angle in 3)	Median, 19.8 mL	Median, 33 mo	100%	Slight worsening of pre-existing V/ XII in 1 (8%)	4 (31%)
Present series	17 (V in 5, IX/X/XI in 7, VII in 4, III in 1)	Mean, 8.2 mL	Median, 59.5 mo	94%	No patient had development of new neurologic deficit	8 (47%)

Abbreviations: V = trigeminal nerve; VII = facial nerve; IX/X/XI = glossopharyngeal nerve/vagus nerve/accessory nerve passing through jugular foramen; XII = hypoglossal nerve; III = oculomotor nerve; N.R. = not reported; II = optic nerve; IV = trochlear nerve; VI = abducent nerve; VIII = vestibulocochlear nerve.

previous series using SRS (8–14) and SRT (20). No patient showed a worsening of pre-existing neurologic symptoms or had new cranial nerve deficits develop. Improvement of pre-

existing neurologic symptoms was seen in 8 patients (47%), which is a relatively high rate in comparison to existing reports (Table 2). No severe complications were observed during

follow-up. In clinical practice facial nerve schwannoma has probably been the most harmful disease among the nonacoustic intracranial schwannomas because of the facial nerve palsy after total resection. However, it was notable that in our series no patients had worsening of their pre-existing neurologic symptoms and 2 patients showed an improvement. Mabanta *et al.* (9) reported that SRS achieved local control of 2 facial nerve schwannomas, although one of these cases had worsening of pre-existing facial nerve palsy. Considering that worsening of facial palsy often induces depression in patients and reduces their quality of life, SRT should be considered an alternative to surgery for patients with facial nerve schwannoma. SRT is at least as effective as SRS and possibly more effective in preserving neurologic function, although the number of patients is too small to compare between SRT and SRS for nonacoustic intracranial schwannoma.

Transient enlargement of schwannoma with cystic change is often seen in patients with acoustic schwannoma (19), but little is known about the phenomenon of nonacoustic schwannoma. We have seen 1 patient with a trigeminal nerve schwannoma who had enlargement of the tumor with cystic

change for as long as 32 months after SRT. Considering that cystic enlargement of acoustic schwannomas is usually transient, there might be a difference between acoustic and nonacoustic intracranial schwannomas with respect to the ability to resolve the cystic degeneration, although the number of patients in this study was too small to reach a conclusion on this matter.

The optimal radiation dose for the nonacoustic intracranial schwannoma is not known. At our institution, we initially used 4 Gy in 1 fraction or 10 Gy in 4 fractions as a stereotactic boost, but its clinical efficacy was not certain. Fifty grays in 25 fractions, which is used for acoustic schwannoma, would be a reasonable dose for nonacoustic intracranial schwannoma as well.

In conclusion, although the number of patients in each group (*i.e.*, different anatomic sites and treatment methods) is small because of the rarity of nonacoustic intracranial schwannomas, SRT can provide long-term tumor control with a low incidence of neurologic complications for nonacoustic intracranial schwannomas, including facial nerve schwannomas.

REFERENCES

- Samii M, Migliori MM, Tatagiba M, *et al.* Surgical treatment of trigeminal schwannomas. *J Neurosurg* 1995;82:711-718.
- Konovalov AN, Spallone A, Mukhamedjanov DJ, *et al.* Trigeminal neurinomas. A series of 111 surgical cases from a single institution. *Acta Neurochir (Wien)* 1996;138:1027-1035.
- Samii M, Babu RP, Tatagiba M, *et al.* Surgical treatment of jugular foramen schwannomas. *J Neurosurg* 1995;82:924-932.
- Tan LC, Bordi L, Symon L, *et al.* Jugular foramen neuromas: A review of 14 cases. *Surg Neurol* 1990;34:205-211.
- Kida Y, Yoshimoto M, Hasegawa T. Radiosurgery for facial schwannomas. *J Neurosurg* 2007;106:24-29.
- Symon L, Cheesman AD, Kawachi M, *et al.* Neuromas of the facial nerve: A report of 12 cases. *Br J Neurosurg* 1993;7:13-22.
- Sanna S, Sekhar LN, Schessel DA. Nonvestibular schwannomas of the brain: A 7-year experience. *Neurosurgery* 2002;50:437-449.
- Pollock BE, Foote RL, Stafford SL. Stereotactic radiosurgery: The preferred management for patients with nonvestibular schwannomas? *Int J Radiat Oncol Biol Phys* 2002;52:1002-1007.
- Mabanta SR, Buatti JM, Friedman WA, *et al.* Linear accelerator radiosurgery for nonacoustic schwannomas. *Int J Radiat Oncol Biol Phys* 1999;43:545-548.
- Sanna M, Bacciu A, Falcioni M, *et al.* Surgical management of jugular foramen schwannomas with hearing and facial nerve function preservation: A series of 23 cases and review of the literature. *Laryngoscope* 2006;116:2191-2204.
- Litre CF, Gourg GP, Tamura M, *et al.* Gamma knife surgery for facial nerve schwannomas. *Neurosurgery* 2007;60:853-859.
- Huang C-F, Kondziolka D, Flickinger JC, *et al.* Stereotactic radiosurgery for trigeminal schwannomas. *Neurosurgery* 1999;45:11-16.
- Martin JJ, Kondziolka D, Flickinger JC, *et al.* Cranial nerve preservation and outcome after stereotactic radiosurgery for jugular foramen schwannomas. *Neurosurgery* 2007;61:76-81.
- Muthukumar N, Kondziolka D, Lunsford LD, *et al.* Stereotactic radiosurgery for jugular foramen schwannomas. *Surg Neurol* 1999;52:172-179.
- Shirato H, Sakamoto T, Sawamura Y, *et al.* Comparison between observation policy and fractionated stereotactic radiotherapy (SRT) as an initial management for vestibular schwannoma. *Int J Radiat Oncol Biol Phys* 1999;44:545-550.
- Kagei K, Shirato H, Suzuki K, *et al.* Small-field fractionated radiotherapy with or without stereotactic boost for vestibular schwannoma. *Radiother Oncol* 1999;50:341-347.
- Fuss M, Debus J, Lohr F, *et al.* Conventionally fractionated stereotactic radiotherapy (FSRT) for acoustic neuromas. *Int J Radiat Oncol Biol Phys* 2000;48:1381-1387.
- Andrews DW, Suarez O, Goldman HW, *et al.* Stereotactic radiosurgery and fractionated stereotactic radiotherapy for the treatment of acoustic schwannomas. Comparative observation of 125 patients treated at one institution. *Int J Radiat Oncol Biol Phys* 2001;50:1265-1278.
- Shirato H, Sakamoto T, Takeichi N, *et al.* Fractionated stereotactic radiotherapy for vestibular schwannoma (VS): Comparison between cystic-type and solid-type VS. *Int J Radiat Oncol Biol Phys* 2000;48:1395-1401.
- Zabel A, Debus J, Thilmann C, *et al.* Management of benign cranial nonacoustic schwannomas by fractionated stereotactic radiotherapy. *Int J Cancer* 2001;96:356-362.
- Day JD, Fukushima T. The surgical management of trigeminal neuromas. *Neurosurgery* 1998;42:233-241.
- Wallner KE, Pitts LH, Davis RL, *et al.* Radiation therapy for the treatment of non-eighth nerve intracranial neurilemmoma. *Int J Radiat Oncol Biol Phys* 1988;14:287-290.

Differential Diagnosis Between Radiation Necrosis and Glioma Progression Using Sequential Proton Magnetic Resonance Spectroscopy and Methionine Positron Emission Tomography

Takeshi NAKAJIMA, Toshihiro KUMABE, Masayuki KANAMORI, Ryuta SAITO, Manabu TASHIRO*, Mika WATANABE**, and Teiji TOMINAGA

Departments of Neurosurgery and **Pathology,
Tohoku University Graduate School of Medicine, Sendai, Miyagi;
*Division of Cyclotron Nuclear Medicine, Tohoku University Cyclotron and
Radioisotope Center, Sendai, Miyagi

Abstract

Differential diagnosis between radiation necrosis and tumor recurrence is important in the clinical management of glioma. Multi-modality imaging including proton magnetic resonance spectroscopy (¹H-MRS) and positron emission tomography (PET) with L-[methyl-¹¹C]methionine (MET) was evaluated. Eighteen patients underwent sequential ¹H-MRS and MET-PET. The expressions of metabolites including choline-containing compounds (Cho), creatine phosphate (Cre), and lactate (Lac) were calculated as the ratios of Cho to Cre (Cho/Cre) and Lac to Cho (Lac/Cho). The uptake of MET was determined as the ratio of the lesion to the contralateral reference region (L/R). The final diagnoses were determined by histological examination and/or follow-up MR imaging and clinical course. The Lac/Cho ratio was 0.63 ± 0.25 (mean \pm standard deviation) in recurrence (7 cases) and 2.35 ± 1.81 in necrosis (11 cases). The Lac/Cho ratio was significantly different between the two groups ($p < 0.01$). Consecutive investigation of ¹H-MRS revealed temporary elevation of Cho in 4 of 9 cases of necrosis, which could be identified as false positive findings for recurrence. Including those cases, MET-PET demonstrated significant difference in the L/R ratio between the two groups (2.18 ± 0.42 vs. 1.49 ± 0.35 , $p < 0.01$). According to a 2×2 factorial table analysis, the borderline values of Lac/Cho and L/R to differentiate recurrence from necrosis were 1.05 and 2.00, respectively. ¹H-MRS is reliable and accessible for the differentiation of recurrence and necrosis, although the temporary elevation of Cho in the course of necrosis should be recognized. Additional MET-PET imaging can establish the diagnosis.

Key words: glioma, necrosis, recurrence, positron emission tomography, proton magnetic resonance spectroscopy

Introduction

Treatment strategy for malignant glioma has become more integrated over the past 10 years, and now incorporates surgical debulking, adjuvant chemotherapy, and various forms of radiation treatment.^{2,11,17,25,26,30} This progress has provided longer survival time for the patients after the initial treatment, but has also given rise to other problems such as differentiation of radiation necrosis from recurrent tumor.^{10,21} The salvage methodology has

not been established, so advances in post-initial treatment may further improve outcome. Several neuroimaging modalities have been assessed for the differential diagnosis of radiation necrosis and tumor recurrence. Thallium-201 single photon emission computed tomography and [¹⁸F]fluorodeoxyglucose (FDG)-positron emission tomography (PET) can predict the malignancy of a tumor before treatment,^{4,7,29} and are sensitive but relatively nonspecific for the differential diagnosis of tumor recurrence and radiation necrosis.^{3,5,16} FDG-PET measurement of regional cerebral metabolism of glucose is useful for the assessment of tumor viability,⁷ but cannot distinguish necrosis from recurrent tumor because

Received January 5, 2009; Accepted March 13, 2009

of the similar affinity for histologically reactive components such as accumulation of macrophages in irradiated brain tissue and recurrent tumor.³⁾ In contrast, L-[methyl-¹¹C]methionine (MET)-PET reflects the metabolism of amino acids in the cell membrane, and is relatively good for discriminating tumor recurrence and radiation necrosis.^{20,28)}

The recent widespread availability of magnetic resonance (MR) imaging and development of image processing sequences including proton MR spectroscopy (¹H-MRS) now allow follow up at short intervals.^{20,28)} The choline signal of ¹H-MRS represents the combined signals from the methyl groups of several molecular species of cytosolic choline-containing compounds (Cho) including glycerophosphocholine, phosphocholine, and choline involved in membrane synthesis and degradation.^{12,18)} Higher Cho signals are a reliable predictor of proliferative activity measured by MIB-1 labeling index in glioma.²²⁾ In contrast, increased Cho signal also reflects accelerated membranous turnover which does not necessarily correlate with proliferative activity.¹²⁾

The present study retrospectively analyzed the clinical use of ¹H-MRS and MET-PET in patients with irradiated glioma to differentiate tumor recurrence and radiation necrosis in the follow-up period.

Materials and Methods

I. Patient population

Eighteen patients, 12 men and 6 women aged 14 to 67 years (mean 45.0 years), had previously received radiochemotherapy for histologically-confirmed glioma (4 diffuse astrocytoma, 6 anaplastic astrocytoma, 8 glioblastoma) and subsequently developed recurrent lesions on MR imaging, suspected to be recurrent tumor or radiation necrosis. The patients periodically underwent clinical and MR imaging examinations, not always including ¹H-MRS, every 2 or 3 months after the initial treatment in our institution. MR imaging including ¹H-MRS was sequentially performed after the recurrent lesion appeared. MET-PET was additionally performed to determine the treatment strategy. The follow-up investigation continued to August 31, 2008. The clinical characteristics of the patients are summarized in Table 1. The protocol was approved by the Clinical Committee of Radioisotope Use of this institution and written informed consent was obtained from each subject in accordance with the guidelines approved by Tohoku University and the Declaration of Human Rights, Helsinki.

Table 1 Characteristics of 18 patients who underwent proton magnetic resonance spectroscopy (¹H-MRS) and methionine positron emission tomography (MET-PET)

Case No.	Age (yrs)/ Sex	Primary diagnosis	¹ H-MRS			MET-PET		Second diagnosis (Cl or Pa)	Present status; Interval from RT (mos)	
			Cho/ Cre	Lac/ Cho	Temporary Cho peak		L/R ratio; Interval from RT (mos)			
					Cho/ Cre	Lac/ Cho				Interval from RT (mos)
1	14/F	A	2.21	0.43			2.13; 80	R (Pa)	DT; 96	
2	63/M	GBM	4.36	0.68			2.24; 8	R (Pa)	DT; 15	
3	56/M	A	3.53	0.49			2.4; 12	R (Pa)	DT; 27	
4	49/M	GBM	2.76	0.3			2.32; 4	R (Pa)	DT; 17	
5	66/M	GBM	2.67	0.87			2.62; 31	R (Pa)	DT; 38	
6	33/F	AA	4.12	0.65			1.3; 54	R (Pa)	DT; 63	
7	23/M	AA	2.57	1.01			2.22; 9	R (Pa)	DT; 25	
8	67/F	A	3.30	1.55	2.93	0.34	12	1.92; 15	N (Pa)	S; 110
9	25/F	GBM	1.43	6.42				0.96; 13	N (Cl)	DT; 22
10	62/M	AA	1.94	4.38	2.24	0.37	8	1.27; 14	N (Cl)	DO; 34
11	58/F	GBM	2.33	1.26				1.74; 29	N (Pa)	DT; 54
12	38/M	A	1.46	1.09	3.32	0.41	16	1.57; 17	N (Cl)	S; 126
13	59/M	GBM	1.41	1.8				1.72; 36	N (Pa)	DO; 50
14	28/M	GBM	no exam	no exam				1.99; 45	N (Pa)	DO; 64
15	31/M	AA	no exam	no exam				1.01; 12	N (Pa)	S; 145
16	67/F	GBM	3.62	1.42				1.26; 11	N (Cl)	DT; 70
17	33/M	AA	2.46	1.66	4.39	0.18	28	1.6; 35	N (Pa)	DT; 88
18	38/M	AA	2.3	1.61				1.35; 11	N (Pa)	S; 158

A: diffuse astrocytoma, AA: anaplastic astrocytoma, Cho: choline-containing compounds, Cl: clinically diagnosed, Cre: creatine phosphate, DO: died of other causes, DT: died of tumor progression, GBM: glioblastoma, Lac: lactate, L/R: ratio of the lesion to the contralateral reference region, N: necrosis, no exam: not examined, Pa: pathologically diagnosed, R: recurrence, RT: radiation therapy, S: survived.

II. Proton MR spectroscopy

Single-voxel point resolved spectroscopy used a 1.5-T whole-body system (Signa; General Electric Medical Systems, Milwaukee, Wis., U.S.A.) and a standard head coil with acquisition parameters of spectral width 2.5 MHz, 2048 data points, repetition time 2000 msec, echo time 272 msec, and averaged over 128 acquisitions. The voxel of interest varied from $12 \times 12 \times 16$ mm to $20 \times 20 \times 20$ mm depending on the lesion size. The size and location of the voxel were carefully adjusted to include a representative part of the lesion enhanced by contrast medium as determined by previously obtained T_1 -weighted MR imaging. T_1 -weighted MR imaging with gadolinium-diethylenetriaminepenta-acetic acid (Gd-DTPA) was then obtained to confirm the spatial relationship between the spectroscopic voxel and the enhanced lesion. Shimming and water suppression were accomplished by automatic software (SA/GE; General Electric Medical Systems). The peaks detected by ^1H -MRS were identified as follows: Cho at 3.2 ppm, creatine phosphate (Cre) at 3.0 ppm, N-acetyl aspartate at 2.0 ppm, and lactate (Lac) at 1.3 ppm. The Lac assignment was made by the formation of the characteristic doublet due to the J coupling and/or inversion of the peak at echo time of 136 msec caused by the J modulation.⁶⁾ The area under the detected peak was measured using software (SA/GE; General Electric Medical Systems). These peak identification and area calculation were manually performed by a single physician who was independent of clinical treatment and unaware of the final differential diagnosis for each subject. The ratios of the peaks such as Cho/Cre and Lac/Cho were used for further statistical analysis.

III. MET-PET

PET used a three-dimensional PET scanner with 32 ring detectors (SET2400W; Shimadzu Inc., Kyoto) to collect data for 10 minutes starting 20 minutes after intravenous bolus injection of 200–550 MBq of MET. The spatial resolution was 3.9 mm at full width at half maximum and the axial field of view was 200 mm. The subjects lay comfortably on the scanner couch with their eyes closed in a dim and quiet environment. Transmission scanning (post-emission transmission) was also performed for 10 minutes using a $^{68}\text{Ge}/^{68}\text{Ga}$ external rotating line source (370 MBq at purchase) to correct the tissue attenuation of emission photons. Acquired data were reconstructed into $128 \times 128 \times 63$ matrix images for a set of three-dimensional volume images by applying a filtered back-projection algorithm using a supercomputer (SX-4/128H4; NEC Corp., Tokyo) at the Synergy Center, Tohoku University. As previ-

ously described,⁹⁾ PET images were semiquantitatively evaluated using irregular regions of interest (ROIs) delineated by an investigator with a thorough knowledge of both nuclear medicine and the clinical characteristics of the patients. Each ROI was manually placed on the lesion (including the pixel with the highest accumulation) and the contralateral region of the normal gray matter as a reference. The L/R ratio was defined as the mean counts of radioisotope per pixel in the lesion ROI divided by the mean counts per pixel in the reference ROI.

IV. Statistical analysis

The calculated Cho/Cre and Lac/Cho ratios from ^1H -MRS, and the L/R ratio from MET-PET in both necrosis and recurrence groups were compared using the Mann-Whitney U-test. Arbitrary values of the Cho/Cre, Lac/Cho, and L/R ratios were used to divide the patients into two groups (high and low groups). A 2×2 factorial table was constructed and the probability values were calculated using Fisher's exact test to verify that the lowest probability values were derived from the borderline values of Cho/Cre, Lac/Cho, and L/R ratios for the necrosis and recurrence groups. All values are expressed as the means \pm standard deviation, unless noted otherwise. The level of significance was defined as a p value of less than 0.05.

Results

Surgical resection or biopsy of the lesion was performed in 14 of the 18 patients. The histological diagnosis was recurrence in 7 patients and necrosis in 7 patients. Radiation necrosis was defined as only irradiated reactive tissue without viable tumor component. Definitive diagnoses of radiation necrosis were established in the other 4 patients on the basis of absence of aggravation or resolution of neurological symptoms, and the neuroimaging findings at more than 6 months after the MET-PET examination. The mean follow-up period was 66.8 months.

Four patients, three with histological necrosis and one with clinical necrosis, were still alive at the end of the follow-up period. Eleven patients, 4 with necrosis and 7 with recurrence, died of tumor progression. The other 3 patients, all with necrosis, died of other causes such as pneumonia or pulmonary embolism. The mean survival time between MET-PET and death of tumor progression was 36.5 months in the 4 patients with necrosis (Cases 9, 11, 16, and 17), and 11.9 months in the 7 patients with recurrence (Cases 1–7).

All patients had parenchymatous mass lesion appearing as low intensity on T_1 -weighted MR imaging

Table 2 Subdivision of calculated values in proton magnetic resonance spectroscopy and methionine positron emission tomography

Diagnosis	No. of patients					
	High Cho/Cre (>2.50)	Low Cho/Cre (<2.50)	High Lac/Cho (>1.05)	Low Lac/Cho (<1.05)	High L/R (>2.00)	Low L/R (<2.00)
Recurrence	6	1	0	7	6	1
Necrosis	2	7	9	0	0	11

Cho: choline-containing compounds, Cre: creatine phosphate, Lac: lactate, L/R: ratio of the lesion to the contralateral reference region.

and high intensity on T₂-weighted MR imaging, with heterogeneous enhancement by Gd-DTPA. These conventional MR imaging sequences could not distinguish between tumor recurrence and radiation necrosis. ¹H-MRS revealed similar mean Cho/Cre ratio of 3.17 ± 0.83 in the patients with recurrent tumor and 2.25 ± 0.80 in the patients with radiation necrosis, with no statistical significance. In contrast, the mean Lac/Cho ratio was significantly lower at 0.63 ± 0.25 in the patients with recurrence compared to 2.35 ± 1.81 in the patients with necrosis (p < 0.01).

The serial ¹H-MRS findings of each patient were also investigated to identify any time-dependent spectral changes. Four of 9 patients with radiation necrosis (Cases 8, 10, 12, and 17) demonstrated temporary increase of the Cho signal, followed by subsequent decrease. The Cho/Cre ratio was 2.93, 2.24, 3.32, and 4.39, and the Lac/Cho ratio was 0.34, 0.37, 0.41, and 0.18 at the temporary increase of the Cho peak (Table 1). No such Cho fluctuation was observed in the other patients.

MET-PET was performed at 4–80 months (mean 24.2 months) after radiation therapy. The mean L/R ratio was 2.18 ± 0.42 (range 1.3–2.62) in the patients with recurrence and 1.49 ± 0.35 (0.96–1.99) in the patients with necrosis, with a significant difference between the two groups (p < 0.01).

The borderline Cho/Cre value of 2.50 provided the lowest probability value of 0.02 for separating the recurrence and necrosis groups. The sensitivity and specificity were 85.7% and 77.8%. The borderline Lac/Cho value of 1.05 resulted in a probability value of less than 0.001. The sensitivity was 100% and specificity was 88.9%. The borderline L/R value of 2.00 provided the lowest probability value of less than 0.001. The sensitivity was 85.7% and specificity was 100% (Table 2).

Illustrative Cases

Case 1: A 14-year-old female with headache and

nausea was admitted to our hospital. MR imaging showed obstructive hydrocephalus and a faintly enhanced mass lesion in the right thalamus (Fig. 1A left). Ventriculoperitoneal shunting and stereotactic biopsy were performed. Histological examination established the diagnosis of diffuse astrocytoma. The patient received local brain radiation with a total dose of 60 Gy and chemotherapy using nimustine hydrochloride (ACNU). Follow-up MR imaging showed contrast enhancement of the lesion 54 months later that subsequently became more intense (Fig. 1A right). ¹H-MRS and MET-PET were performed at 80 months after the radiation therapy. The Cho/Cre, Lac/Cho, and L/R ratios were 2.21, 0.43, and 2.13, respectively (Fig. 1B, C). Our diagnosis was recurrence on the basis of high uptake in MET-PET and elevation of the Cho peak associated with the subtle Lac peak. MR imaging-guided stereotactic biopsy was performed. The histological diagnosis was anaplastic astrocytoma (Fig. 1D). The patient received stereotactic conformal radiotherapy with a total dose of 24 Gy, but regrettably died of tumor progression at the initial site and diffuse leptomeningeal dissemination at 96 months after the initial treatment.

Case 17: A 33-year-old male with anaplastic astrocytoma in the left insulo-opercular region underwent surgical resection and radio-chemotherapy, followed by intravenous administration of ACNU every 2 months for 2 years. The total radiation dose was 72 Gy to the extended local brain using the hyperfractionated method. Follow-up MR imaging revealed heterogeneous enhancement of the mass lesion posterior to the resection cavity 27 months later (Fig. 2A). ¹H-MRS demonstrated elevation of the Cho peak without a Lac peak. The Cho/Cre and Lac/Cho ratios were 4.39 and 0.18, respectively (Fig. 2B middle). Eight months later, the Cho peak demonstrated a slight decrease accompanied by appearance of a Lac peak, resulting in Cho/Cre ratio of 2.46 and Lac/Cho ratio of 1.66 (Fig. 2B right). Simultaneous MET-PET demonstrated the L/R ratio as 1.60

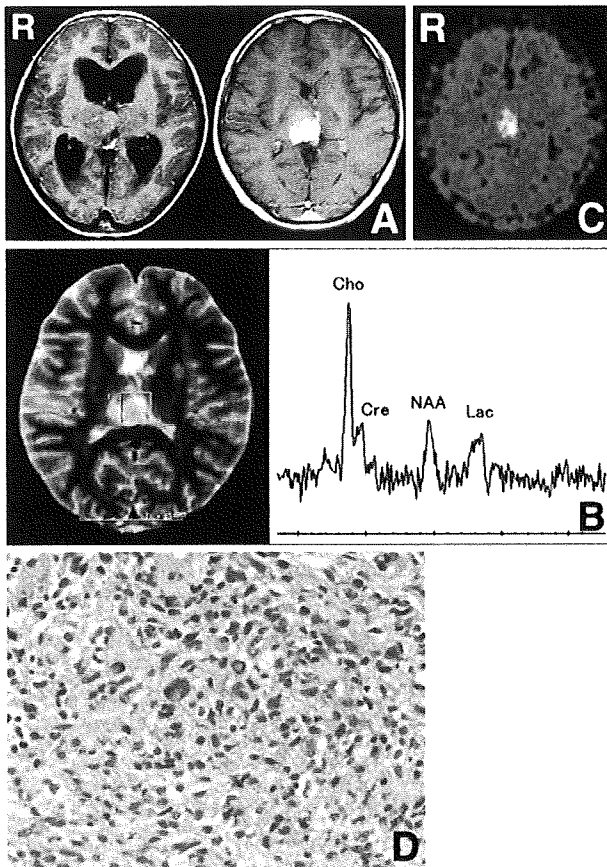


Fig. 1 Case 1: Representative case of recurrence. (A) T₁-weighted magnetic resonance (MR) images with gadolinium-diethylenetriaminepenta-acetic acid showing an enhanced lesion at the first admission (left) and 80 months after the radiation therapy (right). (B) T₁-weighted MR image showing the voxel located within the enhanced lesion (left), and the proton MR spectroscopy spectrum showing elevation of the choline-containing compounds (Cho) peak, decreased N-acetyl aspartate (NAA) peak, and small lactate (Lac) peak (right). Cre: creatine phosphate. (C) L-[methyl-¹¹C]methionine positron emission tomography scan revealing increased uptake in the lesion. The ratio of the lesion to the contralateral reference region is 2.13. (D) Photomicrograph of the tumor specimen showing hypercellular polymorphic viable cells with eosinophilic cytoplasm and hyperchromatic nuclei. Hematoxylin and eosin stain, original magnification $\times 200$.

(Fig. 2C). The MET-PET study did not reveal any intensive accumulation, but the persistent Cho peak indicated total resection of the lesion. Histological

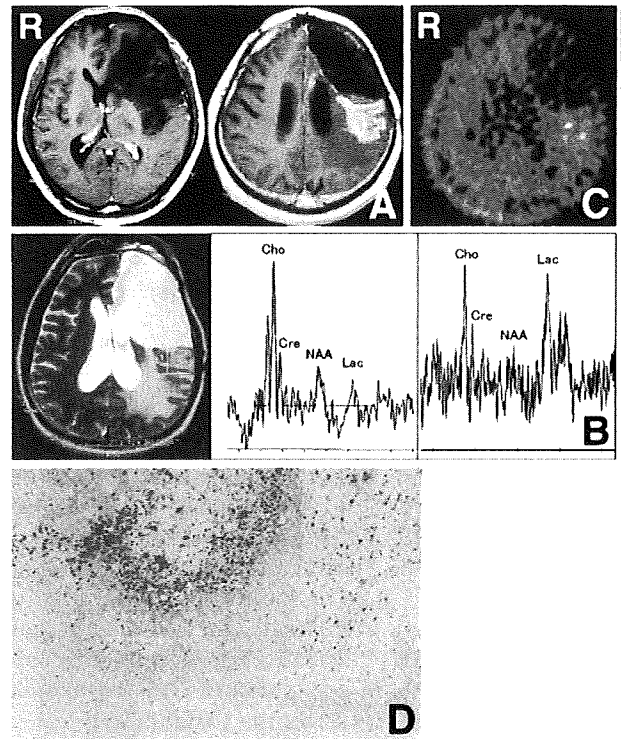


Fig. 2 Case 17: Representative case of radionecrosis. (A) T₁-weighted magnetic resonance (MR) images with gadolinium-diethylenetriaminepenta-acetic acid showing a mass lesion in the left insulo-opercular region at the first admission (left) and 27 months after the radiation therapy (right). (B) T₁-weighted MR image showing the voxel of interest (left), and the proton MR spectroscopy spectra demonstrating elevation of the choline-containing compounds (Cho) peak without a lactate (Lac) peak (center), and decrease of the Cho peak and elevation of the Lac peak, resulting in Cho/creatine phosphate (Cre) ratio of 2.46 and Lac/Cho ratio of 1.66 8 months later (right). NAA: N-acetyl aspartate. (C) L-[methyl-¹¹C]methionine positron emission tomography scan revealing subtle uptake in the lesion. The ratio of the lesion to the contralateral reference region is 1.60. (D) Photomicrograph of the tumor specimen showing coagulation necrosis with partial presence of reactive astrocytes. Hematoxylin and eosin stain, original magnification $\times 100$.

examination resulted in a diagnosis of radiation necrosis with partial presence of reactive astrocytes (Fig. 2D). The patient died of diffuse leptomeningeal dissemination without tumor progression at the initial site at 88 months after the initial treatment.

Discussion

Diffusion-weighted imaging shows radiation necrosis as heterogeneous intensity, whereas recurrent tumor appears as predominantly hyperintensity. Hypointense areas in radiation necrosis are probably liquefactions without polymorphonuclear leukocytes in the chronic necrosis. The maximal value in apparent diffusion coefficient (ADC) maps in necrosis is significantly higher than that in recurrent tumor, but the heterogeneous appearance of radiation necrosis seems to require careful judgment in differential diagnosis.¹⁾ Addition of ADC maps to ¹H-MRS certainly enhanced the discrimination power between pure recurrent tumor and pure necrosis, but did not allow further distinction beyond that provided by ¹H-MRS between specimens of mixed tumor and necrosis, and either pure tumor or pure necrosis.²⁴⁾

¹H-MRS can differentiate recurrent lesion from radiation necrosis after radiation therapy by elevation of the Cho peak.¹⁴⁾ In the present study, ¹H-MRS demonstrated significantly different Lac/Cho ratios in radiation necrosis and recurrence. The borderline Lac/Cho ratio of 1.05 successfully distinguished the two conditions. However, 4 of 9 cases of necrosis demonstrated temporary elevation of the Cho signal that resulted in reduced Lac/Cho ratio. Since lower Lac/Cho value is characteristic of recurrent tumor, this temporary phenomenon might lead to an incorrect diagnosis. Moreover, a previous case of radiation necrosis demonstrated an atypical absence of any characteristic signal.¹⁴⁾ Irradiated brain tissue in the acute phase, within 4 months of treatment, demonstrated increased Cho signal derived from breakdown of the plasma or release of membrane-bound Cho during radiation-induced demyelination.²⁷⁾ In the present study, the temporary elevation of Cho was detected in the chronic phase, but presumably some similar pathogenesis occurred in the lesion. This fluctuation of the Cho signal must be caused by time-dependent changes in metabolism and could influence the findings of ¹H-MRS performed in the acute and chronic periods after radiation therapy. Further clinical experience and investigation will be required for more precise definition of temporary Cho elevation.

MET-PET is useful for differentiating tumorous from nontumorous tissue,¹⁵⁾ correlates with the histological grade of glioma,^{9,23)} and allows biological activity monitoring during the treatment.²⁰⁾ MET-PET is also a sensitive and accurate technique for differentiating between recurrent tumor and radiation necrosis following stereotactic radiosurgery for metastatic brain tumor.²⁸⁾ On the other

hand, high accumulation of MET in brain hematoma and necrotic tissue may be caused by radiation therapy.⁸⁾ Such variations in MET-PET findings seem to depend on the biochemical peculiarity of the radiotracer. The mechanism of the accumulation of MET is not precisely understood, but the metabolism is presumed to reflect protein synthesis, active carrier-mediated transport across the cell membrane, disruption of the blood-brain barrier, high vascular density, and inflammatory response including reactive gliosis.^{13,28)} In the present study, MET-PET could distinguish recurrence and radiation necrosis. Retrospective analysis of the MET-PET findings revealed the borderline L/R ratio could correctly indicate radiation necrosis, even in Cases 8, 10, 12, and 17 with temporary diminution of the Lac/Cho ratio. Furthermore, recurrence was also correctly indicated by the L/R ratio in MET-PET in the present study except for Case 6 who demonstrated low L/R ratio. In this case, the lesion evaluated by MET-PET later vanished but the adjacent Gd-enhanced mass subsequently enlarged and was diagnosed as recurrent lesion by histological examination. Recently, PET with fluoride-labeled boronophenylalanine showed that the coexistence of necrosis and viable recurrence might result in misdiagnosis, which implies the limitation of a single ROI-based study.¹⁹⁾ In general, MET-PET is a powerful tool, especially in patients with false positive indications of ¹H-MRS. This point is the overwhelming advantage of MET-PET despite the high cost and low availability of PET equipment for routine clinical usage.

Conventional MR imaging is basically adequate for the routine examination of patients with glioma after treatment, including radiation therapy, but the emergence of enhanced lesion indicates ¹H-MRS study. Reduction of the Lac/Cho ratio is highly suggestive of recurrent tumor. MET-PET can distinguish recurrence and radiation necrosis, even in the presence of temporary false positive elevation of the Cho peak occurring in radiation necrosis.

References

- 1) Asao C, Korogi Y, Kitajima M, Hirai T, Baba Y, Maki-no K, Kochi M, Morishita S, Yamashita Y: Diffusion-weighted imaging of radiation-induced brain injury for differentiation from tumor recurrence. *AJNR Am J Neuroradiol* 26: 1455-1460, 2005
- 2) Barker FG 2nd, Chang SM, Larson DA, Sneed PK, Wara WM, Wilson CB, Prados MD: Age and radiation response in glioblastoma multiforme. *Neurosurgery* 49: 1288-1297, 2001
- 3) Barker FG 2nd, Chang SM, Valk PE, Pounds TR, Pra-

- dos MD: 18-Fluorodeoxyglucose uptake and survival of patients with suspected recurrent malignant glioma. *Cancer* 79: 115-126, 1997
- 4) Black KL, Hawkins RA, Kim KT, Becker DP, Lerner C, Marciano D: Use of thallium-201 SPECT to quantitate malignancy grade of gliomas. *J Neurosurg* 71: 342-346, 1989
 - 5) Buchpiguel CA, Alavi JB, Alavi A, Kenyon LC: PET versus SPECT in distinguishing radiation necrosis from tumor recurrence in the brain. *J Nucl Med* 36: 159-164, 1995
 - 6) Demaerel P, Johannik K, Van Hecke P, Van Ongeval C, Verellen S, Marchal G, Wilms G, Plets C, Goffin J, Van Calenbergh F: Localized 1H NMR spectroscopy in fifty cases of newly diagnosed intracranial tumors. *J Comput Assist Tomogr* 15: 67-76, 1991
 - 7) Deshmukh A, Scott JA, Palmer EL, Hochberg FH, Gruber M, Fischman AJ: Impact of fluorodeoxyglucose positron emission tomography on the clinical management of patients with glioma. *Clin Nucl Med* 21: 720-725, 1996
 - 8) Dethy S, Goldman S, Blecic S, Luxen A, Levivier M, Hildebrand J: Carbon-11-methionine and fluorine-18-FDG PET study in brain hematoma. *J Nucl Med* 35: 1162-1166, 1994
 - 9) De Witte O, Goldberg I, Wikler D, Rorive S, Damhaut P, Monclus M, Salmon I, Brotchi J, Goldman S: Positron emission tomography with injection of methionine as a prognostic factor in glioma. *J Neurosurg* 95: 746-750, 2001
 - 10) Dooms GC, Hecht S, Brant-Zawadzki M, Berthiaume Y, Norman D, Newton TH: Brain radiation lesions: MR imaging. *Radiology* 158: 149-155, 1986
 - 11) Fine HA, Dear KB, Loeffler JS, Black PM, Canellos GP: Meta-analysis of radiation therapy with and without adjuvant chemotherapy for malignant gliomas in adults. *Cancer* 71: 2585-2597, 1993
 - 12) Fulham MJ, Bizzi A, Dietz MJ, Shih HH, Raman R, Sobering GS, Frank JA, Dwyer AJ, Alger JR, Di Chiro G: Mapping of brain tumor metabolites with proton MR spectroscopic imaging: clinical relevance. *Radiology* 185: 675-686, 1992
 - 13) Ishiwata K, Kubota K, Murakami M, Kubota R, Sasaki T, Ishii S, Senda M: Re-evaluation of amino acid PET studies: can the protein synthesis rates in brain and tumor tissues be measured in vivo? *J Nucl Med* 34: 1936-1943, 1993
 - 14) Kamada K, Houkin K, Abe H, Sawamura Y, Kashiwaba T: Differentiation of cerebral radiation necrosis from tumor recurrence by proton magnetic resonance spectroscopy. *Neurol Med Chir (Tokyo)* 37: 250-256, 1997
 - 15) Lilja A, Lundqvist H, Olsson Y, Spannare B, Gullberg P, Langstrom B: Positron emission tomography and computed tomography in differential diagnosis between recurrent or residual glioma and treatment-induced brain lesions. *Acta Radiol* 30: 121-128, 1989
 - 16) Matheja P, Rickert C, Weckesser M, Hoss N, Schober O: Scintigraphic pitfall: delayed radionecrosis. Case illustration. *J Neurosurg* 92: 732, 2000
 - 17) Matsutani M, Nakamura O, Nagashima T, Asai A, Fujimaki T, Tanaka H, Nakamura M, Ueki K, Tanaka Y, Matsuda T: Intra-operative radiation therapy for malignant brain tumors: rationale, method, and treatment results of cerebral glioblastomas. *Acta Neurochir (Wien)* 131: 80-90, 1994
 - 18) Miller BL: A review of chemical issues in 1H NMR spectroscopy: N-acetyl-L-aspartate, creatine and choline. *NMR Biomed* 4: 47-52, 1991
 - 19) Miyashita M, Miyatake S, Imahori Y, Yokoyama K, Kawabata S, Kajimoto Y, Shibata MA, Otsuki Y, Kirihata M, Ono K, Kuroiwa T: Evaluation of fluoride-labeled boronophenylalanine-PET imaging for the study of radiation effects in patients with glioblastomas. *J Neurooncol* 89: 239-246, 2008
 - 20) Nariai T, Tanaka Y, Wakimoto H, Aoyagi M, Tamaki M, Ishiwata K, Senda M, Ishii K, Hirakawa K, Ohno K: Usefulness of L-[methyl-11C] methionine-positron emission tomography as a biological monitoring tool in the treatment of glioma. *J Neurosurg* 103: 498-507, 2005
 - 21) Ogawa T, Kanno I, Shishido F, Inugami A, Higano S, Fujita H, Murakami M, Uemura K, Yasui N, Mineura K, Kowada M: Clinical value of PET with 18F-fluorodeoxyglucose and L-methyl-11C-methionine for diagnosis of recurrent brain tumor and radiation injury. *Acta Radiol* 32: 197-202, 1991
 - 22) Poptani H, Gupta RK, Roy R, Pandey R, Jain VK, Chhabra DK: Characterization of intracranial mass lesions with in vivo proton MR spectroscopy. *AJNR Am J Neuroradiol* 16: 1593-1603, 1995
 - 23) Ribom D, Eriksson A, Hartman M, Engler H, Nilsson A, Langstrom B, Bolander H, Bergstrom M, Smits A: Positron emission tomography (11C)-methionine and survival in patients with low-grade gliomas. *Cancer* 92: 1541-1549, 2001
 - 24) Rock JP, Scarpace L, Hearshen D, Gutierrez J, Fisher JL, Rosenblum M, Mikkelsen T: Associations among magnetic resonance spectroscopy, apparent diffusion coefficients, and image-guided histopathology with special attention to radiation necrosis. *Neurosurgery* 54: 1111-1117, 2004
 - 25) Sneed PK, Prados MD, McDermott MW, Larson DA, Malec MK, Lamborn KR, Davis RL, Weaver KA, Wara WM, Phillips TL, Gutin PH: Large effect of age on the survival of patients with glioblastoma treated with radiotherapy and brachytherapy boost. *Neurosurgery* 36: 898-903, 1995
 - 26) Stewart LA: Chemotherapy in adult high-grade glioma: a systematic review and meta-analysis of individual patient data from 12 randomised trials. *Lancet* 23: 1011-1018, 2002
 - 27) Szigety SK, Allen PS, Huyser-Wierenga D, Urtasun RC: The effect of radiation on normal human CNS as detected by NMR spectroscopy. *Int J Radiat Oncol Biol Phys* 25: 695-701, 1993
 - 28) Tsuyuguchi N, Sunada I, Iwai Y, Yamanaka K, Tanaka K, Takami T, Otsuka Y, Sakamoto S, Ohata K, Goto

- T, Hara M: Methionine positron emission tomography of recurrent metastatic brain tumor and radiation necrosis after stereotactic radiosurgery: is a differential diagnosis possible? *J Neurosurg* 98: 1056-1064, 2003
- 29) Ueda T, Kaji Y, Wakisaka S, Watanabe K, Hoshi H, Jinnouchi S, Futami S: Time sequential single photon emission computed tomography studies in brain tumor using thallium-201. *Eur J Nucl Med* 20: 138-145, 1993
- 30) van den Bent MJ, Afra D, de Witte O, Ben Hassel M, Schraub S, Hoang-Xuan K, Malmstrom PO, Collette L, Pierart M, Mirimanoff R, Karim AB; EORTC Radiotherapy and Brain Tumor Groups and the UK Medical Research Council: Long-term efficacy of early versus delayed radiotherapy for low-grade astrocytoma and oligodendroglioma in adults: the EORTC 22845 randomised trial. *Lancet* 366: 985-990, 2005

Address reprint requests to: Toshihiro Kumabe, M.D.,
Department of Neurosurgery, Tohoku University
Graduate School of Medicine, 1-1 Seiryō-machi,
Aoba-ku, Sendai 980-8574, Japan.
e-mail: kuma@nsg.med.tohoku.ac.jp

Commentary

We read with great interest the article by Nakajima et al. concerning the distinction between radiation

necrosis and glioma progression. The authors evaluated 18 patients using proton magnetic resonance spectroscopy ($^1\text{H-MRS}$) and positron emission tomography (PET) with L-[methyl- ^{11}C]methionine (MET). The results showed that $^1\text{H-MRS}$ was reliable and accessible for the differentiation of recurrence and necrosis although the temporary elevation of Cho in the course of necrosis should be recognized. Additional MET-PET imaging can distinguish between recurrence and radiation necrosis.

The temporary elevation of Cho pointed out in this study is an interesting phenomenon, which might be related to pseudoprogression in malignant gliomas. Recurrent gliomas seem to be heterogeneous tumors including pure glioma progression, radiation necrosis or both. Furthermore, recurrent gliomas must show change in a time-dependent manner after radiotherapy and chemotherapy. MRS and PET can provide useful metabolic information on this critical issue. Recently, not only methionine but also other tracers, such as fluorothymidine and fluoroethyl-tyrosine, can be used in PET study. In the near future, these multi-imaging modalities may provide accurate important information to distinguish between radiation necrosis and glioma progression.

Takashi TAMIYA, M.D.
Department of Neurological Surgery
Kagawa University Faculty of Medicine
Kagawa, Japan

Gamma Knife radiosurgery for hemangiomas of the cavernous sinus: a seven-institute study in Japan

Clinical article

MASAAKI YAMAMOTO, M.D.,¹ YOSHIHISA KIDA, M.D.,² SEIJI FUKUOKA, M.D.,³
YOSHIYASU IWAI, M.D.,⁴ HIDEFUMI JOKURA, M.D.,⁵ ATSUYA AKABANE, M.D.,⁶
AND TORU SERIZAWA, M.D.⁷

Departments of Neurosurgery, ¹Katsuta Hospital Mito GammaHouse, Hitachi-naka; ²Komaki City Hospital, Komaki; ³Nakamura Memorial Hospital, Sapporo; ⁴Osaka City General Hospital, Osaka; ⁵Furukawa Seiryō Hospital, Oskai; ⁶Kanto Medical Center NTT EC, Tokyo; and ⁷Chiba Cardiovascular Center, Ichihara, Japan

Object. Gamma Knife radiosurgery (GKS) is currently used for primary or postoperative management of cavernous sinus (CS) hemangiomas. The authors describe their experience with 30 cases of CS hemangioma successfully managed with GKS.

Methods. Thirty patients with CS hemangiomas, including 19 female and 11 male patients with a mean age of 53 years (range 19–78 years) underwent GKS at 7 facilities in Japan. Pathological entity was confirmed using surgical specimens in 17 patients, and neuroimaging diagnosis only in 13. Eight patients were asymptomatic before GKS, while 22 had ocular movement disturbances and/or optic nerve impairments. The mean tumor volume was 11.5 cm³ (range 1.5–51.4 cm³). The mean dose to the tumor periphery was 13.8 Gy (range 10.0–17.0 Gy).

Results. The mean follow-up period was 53 months (range 12–138 months). Among the 22 patients with symptoms prior to GKS, complete remission was achieved in 2, improvement in 13, and no change in 7. Hemifacial sensory disturbance developed following GKS in 1 patient. The most recent MR images showed remarkable shrinkage in 18, shrinkage in 11, and no change in 1 patient.

Conclusions. Gamma Knife radiosurgery proved to be an effective treatment strategy for managing CS hemangiomas. Given the diagnostic accuracy of recently developed neuroimaging techniques and the potentially serious bleeding associated with biopsy sampling or attempted surgical removal, the authors recommend that GKS be the primary treatment in most patients who have a clear neuroimaging diagnosis of this condition.

(DOI: 10.3171/2009.6.JNS08271)

KEY WORDS • cavernous sinus • hemangioma • radiosurgery • Gamma Knife

DESPITE past confusion regarding the clinical entity of CS hemangiomas,¹ Gonzalez et al.³ recently reported that this condition is now recognized as a histologically benign vascular tumor with characteristics completely different from those of intracerebral cavernous angiomas, which are vascular malformations. Recent advancements in neuroimaging techniques have allowed precise diagnosis of hemangiomas involving the CS prior to treatment.^{7,16,20} The ideal treatment for CS hemangiomas, whether symptomatic or incidental, has long been total microsurgical resection.⁸ However, because they involve extremely complex anatomical structures and tend to bleed excessively when removed, or even with attempted biopsy sampling, reported surgical results are still unfavorable,^{9,14,21} i.e., relatively low rates of total

removal, though with negligible morbidity rates, even when recently recommended surgical techniques are applied; the extradural approach^{2,17} and induced systemic hypotension.¹¹ For cases in which total removal cannot be achieved, fractionated radiotherapy for the residual tumors has been recommended.¹⁵ At present, GKS is being used for primary or postoperative management of patients with CS hemangiomas and favorable treatment results have been reported.^{5,6,10,12,13,18} However, the incidence of this condition is extremely low. Thus, the small number of reported cases prompted this multiinstitutional analysis of the authors' experiences. Fortunately, GKS is relatively uniform such that treatment techniques using basically the same equipment vary little among institutes. Thus, GKS is considered to be suitable for a multiinstitutional study.

The authors describe 30 patients with CS hemangiomas who were successfully managed with GKS in our 7 institutes in Japan. All 7 facilities started performing

Abbreviations used in this paper: CS = cavernous sinus; GKS = Gamma Knife radiosurgery.

TABLE 1: Summary of characteristics in 30 patients*

Case No.	Age at GKS (yrs), Sex	Initial Presentation	Surgery Pre-GKS	CN Symptoms Pre-GKS	Tumor Vol (cm ³)	Min Dose (Gy)	Length of FU (mos)	Symptom Changes Post-GKS	Most Recent MR Findings
1	33, M	diplopia	no	III	5.2	15.00	30	resolved	remarkable shrinkage
2	54, F	incidental	no	none	3.5	16.00	30	none	remarkable shrinkage
3	44, M	incidental	yes	III	12.3	13.00	50	resolved	shrinkage
4	54, F	incidental	no	none	4.1	13.00	30	none	shrinkage
5	48, M	diplopia	yes	III, IV, V	8.5	13.00	27	improved	no change
6	50, F	ocular pain	no	III, V	1.5	16.20	138	improved	remarkable shrinkage
7	38, F	diplopia	yes	II, VI	3.4	17.00	116	stable	remarkable shrinkage
8	66, F	incidental	yes	II, III, IV, VI	11.1	14.00	83	stable	shrinkage
9	73, F	diplopia	no	II, III	7.7	16.00	78	improved	shrinkage
10	69, F	decreased visual acuity	yes	II, III, IV, V, VI	39.7	10.00	56	stable	shrinkage
11	77, M	ocular pain	yes	III	11.9	13.00	43	stable	shrinkage
12	67, F	diplopia	no	none	19.7	12.50	41	none	shrinkage
13	59, M	decreased visual acuity	yes	II, III	33.4	11.0 × 2†	26	improved	shrinkage
14	46, M	diplopia	yes+RT	none	51.4	15.00‡	84	none	remarkable shrinkage
15	68, F	diplopia	yes	III	6.0	12.00	74	stable	shrinkage
16	54, F	headache	no	none	10.5	15.00	64	none	shrinkage
17	54, F	incidental	yes	none	10.2	15.00	24	none	remarkable shrinkage
18	78, F	diplopia	yes	III	8.5	15.00	52	improved	remarkable shrinkage
19	51, F	diplopia	no	VI	7.9	14.00	26	improved	remarkable shrinkage
20	61, M	diplopia	yes	VI	2.9	16.00	81	improved	remarkable shrinkage
21	45, F	diplopia	no	VI	3.9	15.00	25	improved	remarkable shrinkage
22	46, M	diplopia	no	III	4.9	15.00	13	improved	remarkable shrinkage
23	50, F	diplopia	no	III, IV, VI	19.0	10.00	38	improved	remarkable shrinkage
24	54, F	diplopia	no	III	6.4	16.00	57	improved	remarkable shrinkage
25	35, F	decreased visual acuity	no	II	4.5	12.00	12	improved	remarkable shrinkage
26	19, M	diplopia	yes	none	1.9	14.00	36	none	remarkable shrinkage
27	40, M	diplopia, facial numbness	yes	III, V, VI	5.3	12.00	96	stable	remarkable shrinkage
28	58, F	headache	yes	II	13.6	10.00	52	improved	remarkable shrinkage
29	51, F	diplopia	yes	III	20.8	8.0 × 2†	66	stable	shrinkage
30	56, M	diplopia	yes	none	4.9	12.00	48	none	remarkable shrinkage

* CN = cranial nerve; FU = follow-up; RT = radiation therapy.

† Indicates 2-stage GKS.

‡ Indicates partial coverage.

GKS between 1991 and 1998. Each of the study authors, all of whom are chief neurosurgeons at their facilities, has more than 10 years of GKS experience and each has treated more than 3000 patients with a GK.

Methods

Thirty patients who underwent GKS at 7 GK facilities in Japan and who were followed using MR imaging

for 12 months or more after treatment were studied (Table 1). All patients signed consent forms allowing their data to be used, after the study had been fully explained. Five (Cases 6, 7, 8, 18, and 27) of these 30 patients have been described elsewhere^{5,6,10,13} but are included in this study with further long-term follow-up results. As summarized in Table 1, there were 19 female and 11 male patients with a mean age at the time of GKS of 53 years (range 19–78 years). The most common initial presentation was ocular

Gamma Knife radiosurgery for CS hemangiomas

TABLE 2: Summary of postsurgical changes in symptoms (17 patients)

Preop Symptoms	Ocular Movement Disturbance	Decreased Visual Acuity	Ocular Pain/Headaches	No Deficits	Total (%)
no. of patients	10	2	2	3	17
improved	3	0	0	0	3 (17.6)
no changes	3	0	0	1	4 (23.5)
additional disturbance	4	2	2	2	10 (58.8)

movement disturbances, seen in 18 patients (60.0%). One of the 18 patients had hemifacial sensory disturbance, 4 (13.3%) ocular pain and/or headache, and 3 (10.0%) visual disturbances. The remaining 5 patients were asymptomatic.

Prior to GKS, surgical removal was performed in 17 patients, one of whom underwent postoperative fractionated radiotherapy (Case 14). The nature of the pathological entity was confirmed using surgical specimens in these 17 patients and neuroimaging diagnosis only in 13. Postoperative symptom changes are shown in Table 2. Among 10 patients with ocular movement disturbances, symptom palliation was achieved in 3, there were no changes in 3, and additional neurological deficits developed in the remaining 4. Additional ocular movement disturbances occurred postoperatively in 2 patients with preoperative visual disturbances. Among the remaining 5 patients with no neurological deficits, additional ocular movement disturbances developed postoperatively in 3, and visual disturbance in 1. These postoperative results can be summarized as follows: no neurological deficits before or after surgery in 1 patient (5.9%), improvement in 3 (17.6%), no change in 3 (17.6%), and worsening in 10 patients (58.8%).

Eight patients were asymptomatic before GKS, while 15 had ocular movement disturbances, 2 had optic nerve impairments, and 5 patients had both. The mean tumor volume was 11.5 cm³ (range 1.5–51.4 cm³). Due to the relatively large tumor volumes, staged GKS with intervals of a few weeks was applied in 2 patients (the selected dose at the tumor periphery was 11.0 Gy each time for the patient in Case 13, and 8.0 Gy for the patient in Case 29), and only the tumor base was irradiated in 1 patient (Case 14). In all other patients, the entire tumor volume was fully covered with a 50–60% isodose gradient, and the mean and median doses at the tumor periphery were 13.8 Gy and 14.0 Gy, respectively (range 10.0–17.0 Gy).

Results

All 30 patients underwent periodic MR imaging follow-up. The mean and median follow-up periods after GKS were 53 and 49 months, respectively (range 12–138 months). The most recent MR images demonstrated remarkable tumor shrinkage (> 50% tumor volume reduction) in 18 patients (60.0%), slight shrinkage in 11 (36.7%)

TABLE 3: Summary of postradiosurgical changes in symptoms (30 patients)

Symptoms Pre-GKS	Ocular Movement Disturbance	Decreased Visual Acuity	Both*	No Deficits	Total (%)
no. of patients	15	2	5	8	30
recovery	2*	0	0	0	2† (6.7)
improved	9	2	2	0	13 (43.3)
no changes	4	0	3	8	15 (50.0)
additional disturbance	1†	0	0	0	1† (3.3)

* Indicates both ocular movement disturbance and decreased visual acuity.

† Ocular movement recovered completely but additional trigeminal nerve disturbance occurred in 1 patient.

and no change in 1 (3.3%). No tumors showed transient enlargement after GKS. In the 18 tumors in which remarkable shrinkage was attained, a marked tumor volume decrease had occurred by 12 months after GKS. To date, no patients have experienced tumor recurrence.

Post-GKS changes in neurological symptoms are listed in Table 1 and summarized in Table 3. Among the 20 patients with ocular movement disturbances, including 5 who also had visual disturbances, complete remission of symptoms was obtained in 2, improvement in 12, and no change in 6. Additional trigeminal nerve disturbance occurred in 1 patient (Case 3). Among the 7 patients with visual disturbances (including the 5 with ocular movement disturbances), improvement was noted in 4 and no change in 3. Thus, among the 22 patients with cranial neuropathy before GKS, complete remission was achieved in 2 (9.1%), improvement in 13 (59.1%), and no change in 7 (31.8%). No additional disturbances occurred in the remaining 8 patients who did not have neurological deficits before GKS.

Illustrative Cases

Case 14

Presentation and First Operation. In 1982, an ophthalmologist recommended further examination after this 29-year-old man presented with diplopia. At another institution, neurological examination revealed left oculomotor nerve paresis and a left CS tumor was demonstrated on CT. The patient received a preoperative diagnosis of meningioma and underwent craniotomy, despite failed biopsy sampling due to massive bleeding. The patient's symptoms subsided after steroid treatment.

Second Operation. In 1995, left oculomotor nerve paresis recurred and MR images obtained on January 17, 1996, demonstrated the presence of a left CS tumor extending into the middle fossa (Fig. 1A). The patient underwent a left frontotemporal craniotomy followed by biopsy sampling. Because of massive hemorrhaging, however,

TABLE 4: Summary of the 16 cases reported in the literature*

Authors & Yr	Age at GKS (yrs), Sex	CN Symptoms Pre-GKS	Tumor Vol (cm ³)	Min Dose (Gy)	Length of FU (mos)	Symptom Changes Post-GKS	Tumor Vol at Latest FU (cm ³)	Vol Reduction Rate (%)
Iwai et al., 1999	40, M	III, V, VI	5.3	12.0	20	no change	shrinkage	NA
Thompson et al., 2000	24, F	III	5.6	14.0	24	improved	0.8	14
	14, F	V, VI, VII	5.2	19.0	18	improved	0.9	17
	44, M	III, IV	10.8	15.0	12	improved	10.9	101
Seo et al., 2000	79, F	III, IV	8.5	15.0	24	recovery	shrinkage	NA
Kida et al., 2001	50, F	III, V	1.5	16.2	33	no change	0.7	47
	38, F	II, VI	3.4	17.0	36	improved	1.4	41
	66, F	II, III, IV, VI	11.1	14.0	12	no change	5.1	46
Nakamura et al., 2002	75, F	II, III	9.5	12.0–14.0†	60	improved	4.3	45
	68, F	II	3.3	12.0–14.0†	48	no change	3.0	91
	55, F	none	6.6	12.0–14.0†	24	none	4.6	70
Peker et al., 2004	39, F	none	3.8	15.0	52	none	1.5	39
	60, M	III	5.8	16.0	32	no change	2.1	36
	37, M	V, VI	6.2	15.0	45	improved	1.3	21
	39, F	III, V	4.6	15.0	29	improved	1.1	24
	44, M	II, III	4.4	14.0	6	no change	1.7	39

* NA = not applicable.

† The selected dose for the individual patient was not described.

an attempt at tumor removal had to be discontinued. The pathological report was consistent with a hemangioma. Postoperatively, the patient received fractionated radiotherapy with a total dose of 51 Gy, and significant tumor shrinkage was noted on follow-up MR imaging (Fig. 1B). His oculomotor function gradually improved after radiotherapy, eventually normalizing.

Gamma Knife Radiosurgery. Although there was no neurological deterioration, MR images obtained 60 months posttreatment demonstrated apparent regrowth of the tumor (Fig. 1C). The patient underwent GKS at the Katsuta Hospital Mito GammaHouse on January 19, 2000. Because of prior radiotherapy and a relatively large tumor volume (51.4 cm³) the lower half of the tumor was covered with a 50% isodose gradient and irradiation was administered with the maximum dose of 30.0 Gy; that is, 56% of the entire tumor received a radiation dose of ≥ 15.0 Gy. The patient's neurological status has been stable since radiosurgery. Follow-up MR images obtained 6 months after GKS revealed remarkable shrinkage through the 12th postradiosurgical month and confirmed the absence of growth thereafter up to the most recent follow-up MR imaging studies obtained 84 months after radiosurgery (Figs. 1D and E and 2).

Case 15

This 68-year-old woman presented with a 3-month history of diplopia, and further examination was recommended by the ophthalmologist. At another institution (not one of the 7 GKS institutions), neurological examination revealed right oculomotor nerve paresis and a right CS tumor was demonstrated on MR imaging. Bi-

opsy sampling through a frontotemporal craniotomy was performed, and the lesion was confirmed to be consistent with a hemangioma.

The patient underwent GKS at the Katsuta Hospital Mito GammaHouse on August 7, 2001. The tumor, with a volume of 6.0 cm³, was covered with a 60% isodose gradient and irradiated with a peripheral dose of 12.0 Gy (Fig. 3A). Postradiosurgically, to date, her oculomotor nerve function has remained unchanged. Follow-up MR images obtained 6 months after GKS showed a slight shrinkage of the lesion that continued through the 12th postradiosurgical month, and absence of growth was confirmed thereafter up to the most recent follow-up MR imaging, conducted 74 months after GKS (Fig. 3B and C).

Case 16

This 54-year-old woman presented to an outside institution with a 2-month history of headaches. Neuroimaging examinations showed typical findings of a hemangioma involving the left CS. Her headaches were nonspecific and not considered to be caused by the tumor. Therefore, a watch and wait approach was recommended. However, the patient was extremely concerned about not being treated, and GKS was therefore undertaken at Katsuta Hospital Mito GammaHouse on February 9, 2002. The tumor, with a volume of 10.5 cm³, was covered with a 60% isodose gradient and irradiated with a maximum dose of 25.0 Gy (the entire tumor received an irradiation dose of 15.0 Gy or more; Fig. 4 left). Periodic follow-up MR images showed slight shrinkage. No growth has been seen to date, with the most recent follow-up MR images having been obtained 64 months after radiosurgery (Fig. 4 right).

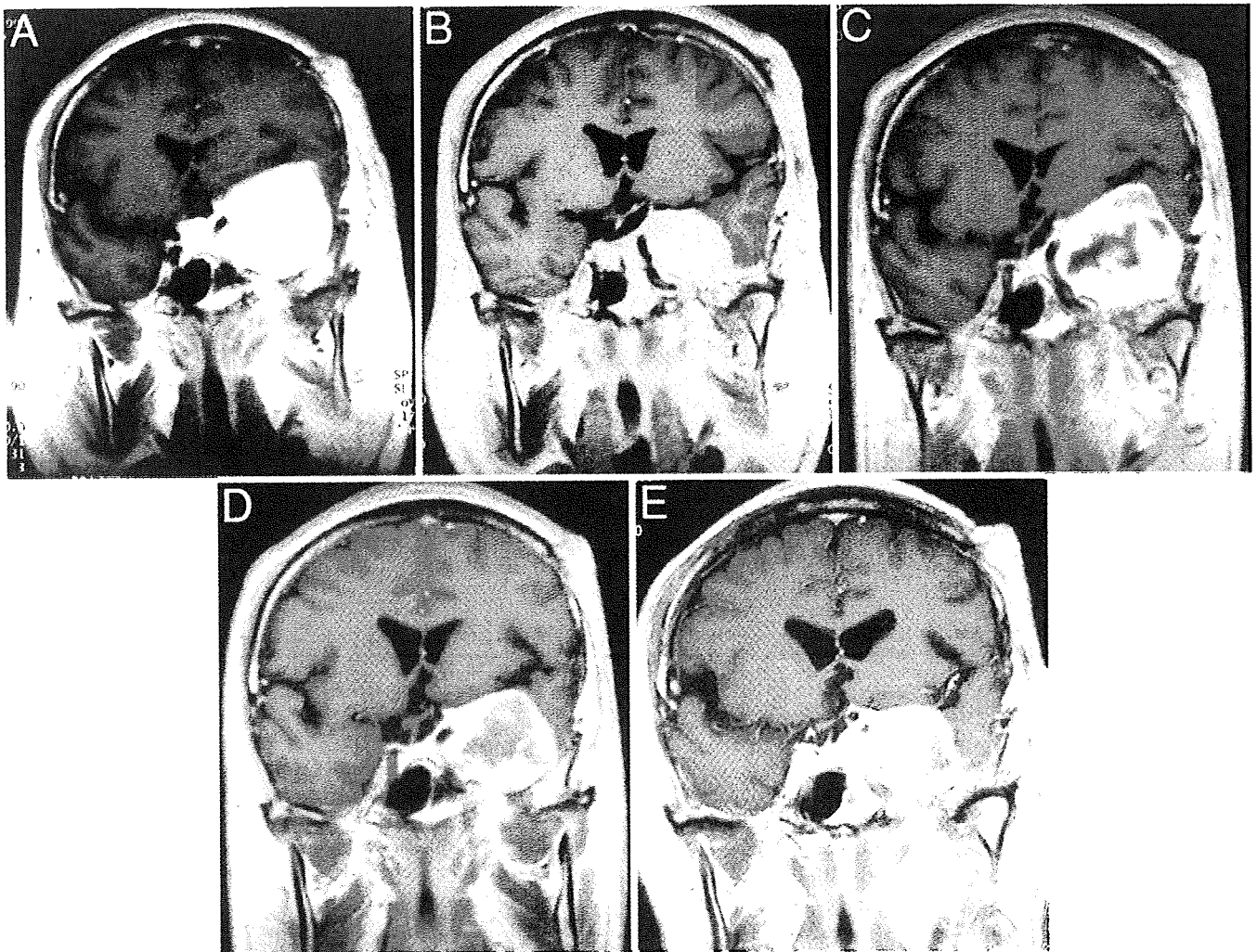


FIG. 1. Case 14. Sequential contrast-enhanced coronal T1-weighted MR images obtained before the second surgery and radiation therapy (A), 31 months after treatment (B), 60 months after these treatments but before GKS (C), and 12 (D) and 84 months after GKS (E).

Discussion

Since the first patient with a CS hemangioma who underwent successful treatment with GKS was described (Case 27 in this article),⁵ 16 cases have been reported in the literature (Table 4).^{5,6,10,12,13,18} These 16 cases have included 11 female and 5 male patients with a mean age of 48 years (range 14–79 years) at the time of GKS, and a mean tumor volume of 6.0 cm³ (range 1.5–11.1 cm³). Selected doses at the tumor periphery have ranged from 12.0 to 19.0 Gy, with a mean and median of 14.8 and 15.0 Gy, respectively. Magnetic resonance images obtained 6–60 months (mean 30, median 27 months) after GKS demonstrated tumor shrinkage in 14 patients and no change in 2. Excluding 2 patients in whom the tumor volume on the most recent MR imaging studies was not available, postradiosurgical volume reduction rates ranged from 14 to 101% (mean and median of 45 and 40%, respectively). Among the 14 of these 16 patients with cranial nerve impairments prior to GKS, complete resolution was achieved in 1 patient, improvement in 7, and in 6 these

impairments remained essentially unchanged. No additional symptoms occurred in any of these 16 patients reported in the literature.

In these previously reported cases, however, postradiosurgical follow-up periods were not sufficiently long: the follow-up period was \leq 36 months in 12 (75.0%) of the 16 patients, and the maximum was 60 months. In the present study of 30 patients, 19 (63.3%) underwent post-GKS follow-up for 3 years or longer, and 10 (33.3%) for 5 years or longer, with a maximum of 138 months. Even in the group of patients with a longer follow-up period, good control of tumor growth was obtained.

We analyzed dose-treatment responses based on 38 cases: 27 of the 30 cases we reported here (the 2 with staged GKS and 1 with partial coverage were excluded) plus 11 previously reported cases. Duplicate citations were avoided.^{5,6,10,13} As shown in Fig. 5, there was a tendency for remarkable tumor shrinkage (volume reduction rates of \geq 50% relative to those before GKS) in the tumors receiving higher doses. Remarkable shrinkage was demon-

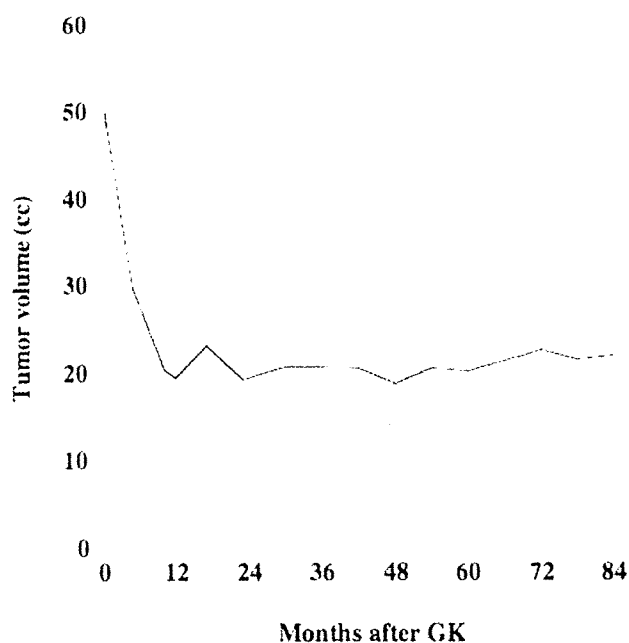


Fig. 2. Case 14. Graph showing postradiosurgical volume changes in this patient.

strated in 15 (83.3%) of 18 tumors that received radiation doses of ≥ 15 Gy, and in 10 of the 20 lesions that received < 15 Gy (not statistically significant; $p = 0.0377$). On the other hand, remarkable tumor shrinkage was demonstrated even in tumors irradiated with relatively low doses: 2 (66.7%) of 3 tumors that received 10.0 Gy, and 3 (60.0%) of 5 that received 12.0 Gy showed shrinkage. We divided these 38 cases into 3 groups based on treatment response shown on the most recent MR images available. Remarkable shrinkage was seen in 25 cases, some shrinkage in 10, and no change in 3. The doses delivered to the tumor periphery differed little among the 3 groups (no statistically significant difference). It can be concluded that a peripheral dose of 14–15 Gy is sufficient to control the growth of CS hemangiomas and that a dose of 10.0–12.0 Gy is the threshold level for tumor growth control.

Although fractionated radiosurgery, also known as stereotactic radiotherapy, is commonly performed for benign intracranial lesions at facilities using a linear accelerator-based radiosurgery system,⁴ it is performed only rarely at GKS facilities. Debate continues as to whether stereotactic radiotherapy and staged radiosurgery are effective and safe for benign lesions. In the 2 patients we have described in the present study who underwent staged radiosurgery, good control of tumor growth was observed at 26 and 66 months using a 2-stage GKS technique with doses at the tumor periphery of 11.0 and 8.0 Gy, respectively. On the other hand, as we have described in detail, only the lower half of the tumor was irradiated with a dose of 15.0 Gy in 1 patient, and tumor growth has been well-controlled for 84 months to date. This technique has been applied to relatively large meningiomas,¹⁹ and the treatment concept assumes that the blood supply from the tumor base can be reduced, allowing tumor growth to be controlled (radiosurgical thrombolization). According to a hypothesis proposed by Linskey et al.,⁸ most small CS hemangiomas are supplied with blood by the meningeal tributaries of the intracavernous carotid artery, and in cases in which the tumors extend toward the middle fossa, there is an additional blood supply from the middle meningeal and accessory middle meningeal arteries. Though we have only 1 such case, the achievement of tumor growth control using radiosurgical thrombolization can be considered to support this hypothesis. Although a final conclusion awaits further experiences, either staged radiosurgery or radiosurgical thrombolization can be applied to relatively large CS hemangiomas.

Conclusions

The GKS treatment results for CS hemangiomas we report in the present study are more favorable than those previously reported after surgical removal.^{9,14,21} Therefore, if a tumor shows clear neuroimaging characteristics of CS hemangioma, and the lesion is small, without evidence either of meningioma or schwannoma, GKS can be performed as the primary treatment procedure.

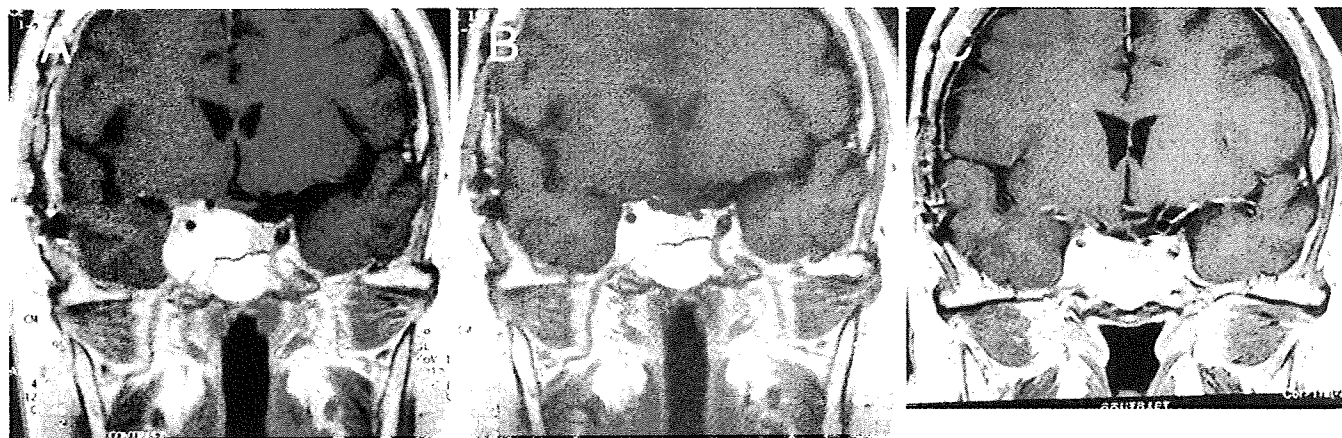


Fig. 3. Case 15. Sequential contrast-enhanced T1-weighted coronal MR images obtained before (A), and 12 (B) and 74 months after GKS (C).

Gamma Knife radiosurgery for CS hemangiomas

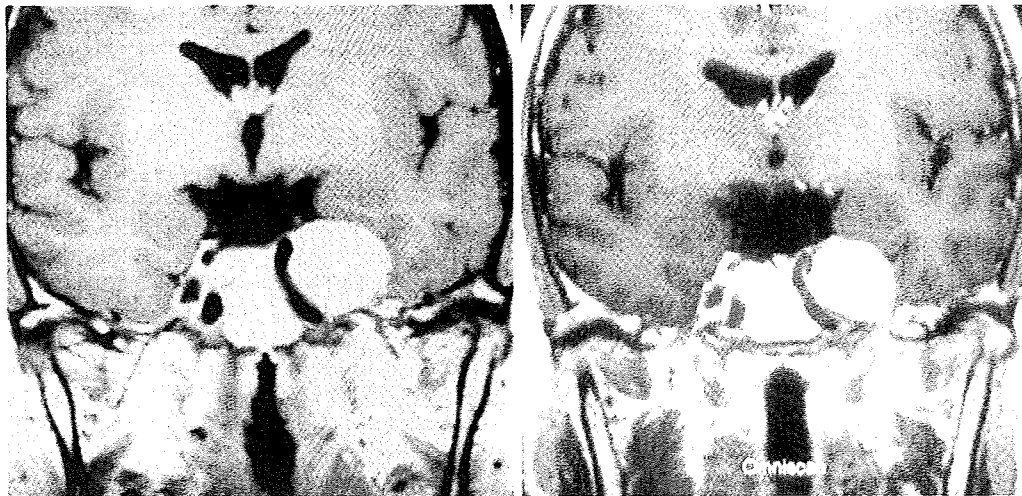


FIG. 4. Case 16. Sequential contrast-enhanced T1-weighted coronal MR images obtained before (*left*) and 64 months after GKS (*right*).

Disclaimer

The authors report no conflict of interest concerning the materials or methods used in this study or the findings specified in this paper.

Acknowledgments

The authors are very grateful to Dr. Nobuhiko Aoki, Department

of Neurosurgery, Tokyo Metropolitan Fuchu Hospital, for the pre- and postsurgical MR images for Case 14. The authors also thank Dr. Makoto Tsuruoka, Department of Neurosurgery, Toride Kyodo Hospital, for the postradiosurgical MR images for Case 17. Finally, the authors express their sincere gratitude to Bierta E. Barford, M.D., Katsuta Hospital Mito GammaHouse, for her outstanding help in preparing this English manuscript.

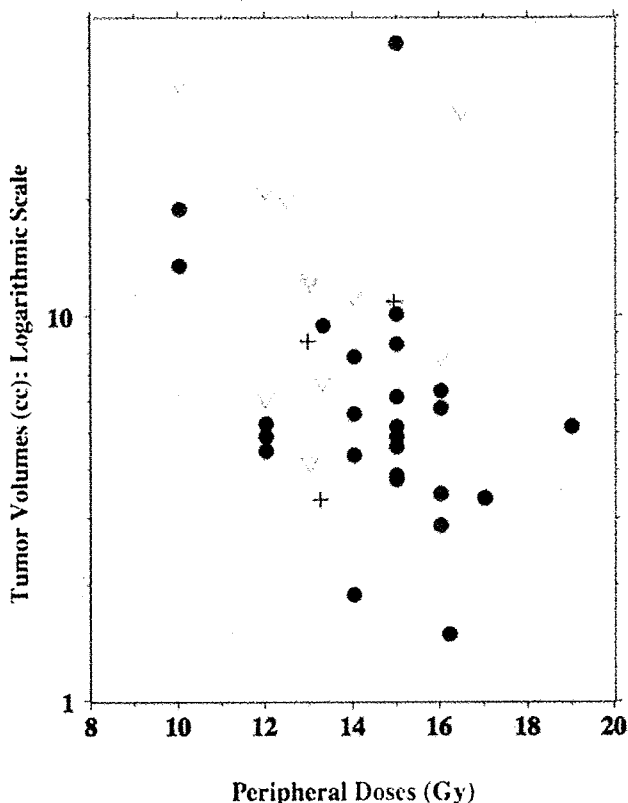


FIG. 5. Scatter plot showing dose, tumor volume, and treatment response. *Circles* indicate remarkable shrinkage, *triangles* indicate some shrinkage, and *plus signs* indicate no change.

References

- Biondi A, Clemenceau S, Dormont D, Deladoeuille M, Ricciardi GK, Mokhtari K, et al: Intracranial extra-axial cavernous (HEM) angiomas: tumors or vascular malformations? *J Neuroradiol* **29**:91–104, 2002
- Goel A, Muzumdar D, Sharma P: Extradural approach for cavernous hemangioma of the cavernous sinus: experience with 13 cases. *Neurol Med Chir (Tokyo)* **43**:112–118, 2003
- Gonzalez LF, Lekovic GP, Eschbacher J, Coons S, Porter RW, Spetzler RF: Are cavernous sinus hemangiomas and cavernous malformations different entities? *Neurosurg Focus* **21** (1):E6, 2006
- Grosu AL, Nieder C: Stereotactic fractionated radiotherapy for recurrent capillary hemangioma of the cavernous sinus. *Strahlenther Onkol* **182**:179–182, 2006
- Iwai Y, Yamanaka K, Nakajima H, Yasui T: Stereotactic radiosurgery for cavernous sinus cavernous hemangioma: case report. *Neurol Med Chir (Tokyo)* **39**:288–290, 1999
- Kida Y, Kobayashi T, Mori Y: Radiosurgery of cavernous hemangiomas in the cavernous sinus. *Surg Neurol* **56**:117–122, 2001
- Latchaw RE, Rothfus WE, Mitchell SL: Imaging of the orbit and its contents, in Wilkins RH, Rengachary SS (eds): *Neurosurgery*, ed 2. New York: McGraw-Hill, 1996 pp 1465–1480
- Linskey ME, Sekhar LN: Cavernous sinus hemangioma: a series, a review, and a hypothesis. *Neurosurgery* **30**:101–107, 1992
- Meyer FB, Lombardi D, Scheithauer B, Nichols DA: Extra-axial cavernous hemangiomas involving the dural sinuses. *J Neurosurg* **73**:187–192, 1990
- Nakamura N, Shin M, Tago M, Terahara A, Kurita H, Nakagawa K, et al: Gamma knife radiosurgery for cavernous hemangiomas in the cavernous sinus. Report of three cases. *J Neurosurg* **97** (5 Suppl):477–480, 2002

11. Ohata K, El-Naggar A, Tamaki T, Morino M, El-Adawy Y, El-Sheik K, et al: Efficacy of induced hypotension in the surgical treatment of large cavernous sinus cavernomas. **J Neurosurg** **90**:702–708, 1999
12. Peker S, Kilic T, Sengoz M, Pamir MN: Radiosurgical treatment of cavernous sinus cavernous haemangiomas. **Acta Neurochir (Wien)** **146**:337–341, 2004
13. Seo Y, Fukuoka S, Sasaki T, Takanashi M, Hojo A, Nakamura H: Cavernous sinus hemangioma treated with gamma knife radiosurgery: usefulness of SPECT for diagnosis: Case report. **Neurol Med Chir (Tokyo)** **40**:575–580, 2000
14. Shi J, Hang C, Pan Y, Liu C, Zhang Z: Cavernous hemangiomas in the cavernous sinus. **Neurosurgery** **45**:1308–1314, 1999
15. Shibata S, Mori K: Effect of radiation therapy on extracerebral cavernous hemangioma in the middle fossa. **J Neurosurg** **67**:919–922, 1987
16. Sohn CH, Kim SP, Kim IM, Lee JH, Lee HK: MR imaging findings of cavernous hemangiomas in the cavernous sinus. **AJNR Am J Neuroradiol** **24**:1148–1151, 2003
17. Suri A, Ahmad FU, Mahapatra AK: Extradural transcavernous approach to cavernous sinus hemangiomas. **Neurosurgery** **60**:483–488, 2007
18. Thompson TP, Lunsford LD, Flickinger JC: Radiosurgery for hemangiomas of the cavernous sinus and orbita: technical case report. **Neurosurgery** **47**:778–783, 2000
19. Yamamoto M, Kamiyo T, Barfod BE, Urakawa Y: Gamma knife radiosurgery for relatively large meningiomas: an interim result. **Neurol Med Chir** (Abstract #03A0544609)
20. Yao Z, Feng X, Chen X, Zee C: Magnetic resonance imaging characteristics with pathological correlation of cavernous malformation in cavernous sinus. **J Comput Assist Tomogr** **30**:975–979, 2006
21. Zhou LF, Mao Y, Chen L: Diagnosis and surgical treatment of cavernous sinus hemangiomas: an experience of 20 cases. **Surg Neurol** **60**:31–36, 2003

Manuscript submitted April 9, 2008.

Accepted June 23, 2009.

Please include this information when citing this paper: published online July 17, 2009; DOI: 10.3171/2009.6.JNS08271.

Address correspondence to: Masaaki Yamamoto, M.D., Katsuta Hospital Mito GammaHouse 5125-2 Nakane, Hitachi-naka Ibaraki 312-0011 Japan. email: BCD06275@nifty.com.

Long-term control of disseminated pleomorphic xanthoastrocytoma with anaplastic features by means of stereotactic irradiation

Tomoyuki Koga, Akio Morita, Keisuke Maruyama, Minoru Tanaka, Yasushi Ino, Junji Shibahara, David N. Louis, Guido Reifenberger, Jun Itami, Ryusuke Hara, Nobuhito Saito, and Tomoki Todo

Departments of Neurosurgery (T.K., A.M., K.M, M.T., Y.I., N.S., T.T.) and Pathology (J.S.), University of Tokyo Hospital, Tokyo, Japan; Department of Pathology, Massachusetts General Hospital, Boston, MA, USA (D.N.L.); Department of Neuropathology, Heinrich-Heine-University, Düsseldorf, Germany (G.R.); Department of Radiation Therapy and Oncology, International Medical Center of Japan, Tokyo, Japan (J.I., R.H.)

Pleomorphic xanthoastrocytoma (PXA) is a rare astrocytic neoplasm of the brain. Some PXAs are accompanied by anaplastic features and are difficult to manage because of frequent recurrences that lead to early death. No previous reports have demonstrated consistent efficacy of adjuvant radiotherapy or chemotherapy for this disease. We report a case of PXA with anaplastic features treated with stereotactic irradiation (STI) that resulted in long-term control of repeatedly recurring nodules throughout the neuraxis. A 47-year-old woman presented with an epileptic seizure due to a large tumor in the right frontal lobe. The tumor was resected and diagnosed as PXA with anaplastic features. Sixteen months later, a relapse at the primary site was noted and treated with stereotactic radiosurgery using Gamma Knife. Two years later, the patient developed a tumor nodule in the cervical spinal cord that histologically corresponded to a small-cell glioma with high cellularity and prominent *MIB-1* (mindbomb homolog 1) labeling. In the following months, multiple nodular lesions appeared through-

out the CNS, and STI was performed six times for eight intracranial lesions using Gamma Knife and twice using a linear accelerator, for three spinal cord lesions in total. All lesions treated with STI were well controlled, and the patient was free from symptomatic progression for 50 months. However, diffuse dissemination along the craniospinal axis eventually progressed, and she died 66 months after initial diagnosis. Autopsy showed that the nodules remained well demarcated from the surrounding nervous system tissue. STI may be an effective therapeutic tool for controlling nodular dissemination of PXA with anaplastic features. *Neuro-Oncology* 11, 446–451, 2009 (Posted to *Neuro-Oncology* [serial online], Doc. D08-00090, January 22, 2009. URL <http://neuro-oncology.dukejournals.org>; DOI: 10.1215/15228517-2008-112)

Keywords: glioma, pleomorphic xanthoastrocytoma, stereotactic irradiation, stereotactic radiosurgery

Pleomorphic xanthoastrocytoma (PXA) is a rare tumor accounting for less than 1% of all astrocytic neoplasms.^{1–4} Maximum surgical removal is considered the first treatment of choice.¹ The efficacy of adjuvant radiotherapy or chemotherapy has not yet been established, largely because of the relative rarity of this disease.^{2,5–7} PXA belongs to grade II of the WHO histological classification of tumors of the CNS and is

Received April 10, 2008; accepted November 26, 2008.

Address correspondence to Tomoki Todo or Tomoyuki Koga, Department of Neurosurgery, University of Tokyo Hospital, 7-3-1 Hongo, Bunkyo-ku, Tokyo 113-8655 Japan (toudou-nsu@umin.ac.jp or kougatky@umin.ac.jp).

Copyright 2009 by the Society for Neuro-Oncology